Current-induced spin-wave Doppler shift and attenuation in compensated ferrimagnets

Dong-Hyun Kim,[1] Se-Hyeok Oh,[2] Dong-Kyu Lee,[3] Se Kwon Kim,[4] and Kyung-Jin Lee [3,4,5,*]

[1]*Department of Semiconductor Systems Engineering, Korea University, Seoul 02841, Korea*
[2]*Department of Nano-Semiconductor and Engineering, Korea University, Seoul 02841, Korea*
[3]*Department of Materials Science and Engineering, Korea University, Seoul 02841, Korea*
[4]*Department of Physics, Korea Advanced Institute of Science and Technology, Daejeon 34141, Korea*
[5]*KU-KIST Graduate School of Converging Science and Technology, Korea University, Seoul 02841, Korea*

We theoretically and numerically study current-induced modification of ferrimagnetic spin-wave dynamics when an electrical current generates adiabatic and nonadiabatic spin-transfer torques. We find that the sign of the Doppler shift depends on the spin-wave handedness because the sign of spin polarization carried by spin waves depends on the spin-wave handedness. It also depends on the sign of the adiabatic-torque coefficient, originating from unequal contributions from two sublattices. For a positive nonadiabaticity of spin current, the attenuation lengths of both right- and left-handed spin waves increase when electrons move in the same direction with spin-wave propagation. Our result establishes a way to simultaneously measure important material parameters of a ferrimagnet, such as angular momentum compensation point, spin polarization, and nonadiabaticity using current-induced control of ferrimagnetic spin-wave dynamics.

I. INTRODUCTION

Conventional semiconductor devices use the electron charge to compute and store information, which inevitably causes Joule heating. In contrast, spin wave (SW) devices, where the SW is used as the information carrier, avoid the Joule heating as the SW is a collective low-energy magnetic excitation that does not involve moving charges [1–3]. Several concepts of SW devices implementing Boolean/non-Boolean computing and multi-input/output operations have been reported [4–17]. Up until now, most SW studies have focused on ferromagnetic SWs.

In comparison to ferromagnetic SWs, antiferromagnetic SWs have several distinct features. Unlike ferromagnetic SWs whose frequency is in gigahertz (GHz) ranges, the frequency of antiferromagnetic SWs can reach terahertz (THz) ranges [18,19], which allows fast SW operation. In addition, both right-handed and left-handed modes are allowed in antiferromagnets because of the antiferromagnetic coupling between two sublattice moments [20,21]. This gives an additional degree of freedom for SW operations [22–26] as compared to the ferromagnetic SW that has only the right-handed mode.

This intriguing antiferromagnetic dynamics is also realized in compensated ferrimagnets [27–40]. Antiferromagnetically coupled ferrimagnets composed of rare-earth (RE) and transition metal (TM) elements have two compensation points. One is the magnetic moment compensation point where the net magnetic moment is zero and the other is the angular momentum compensation point where the net angular momentum is zero. These two compensation points are different when the Landé g factors of RE and TM elements are different [27]. As the intrinsic dynamics of localized spins is governed by the commutation relation between angular momentum (not magnetic moment) and the relevant Hamiltonian, antiferromagneticlike spin dynamics is realized at the angular momentum compensation point of compensated ferrimagnets. Given that the net magnetic moment is nonzero at the angular momentum compensation point, RE-TM ferrimagnets allow us to investigate antiferromagneticlike spin dynamics with a finite Zeeman coupling. For this reason, antiferromagneticlike spin dynamics of compensated ferrimagnets has been extensively studied in recent studies [27–40].

Another intriguing feature of compensated ferrimagnets is that spin transport is distinct from both ferromagnets and antiferromagnets. When a spin-polarized current is injected into a magnetic material, it exerts a torque on the local magnetic moment by transferring spin angular momentum. This spin-transfer torque (STT) [41,42] consists of two mutually orthogonal vector components, adiabatic torque and nonadiabatic torque [43–51], for continuously varying spin textures such as SW, domain wall, and skyrmion. For ferromagnets, it is well known that the adiabatic STT causes current-induced SW Doppler shift [52,53] whereas the nonadiabatic STT controls SW attenuation [54–56]. It was predicted [57] that the current-induced SW Doppler shift by the adiabatic STT is also present for antiferromagnets. Although there has been no study on the current-controlled SW attenuation for antiferromagnets, a recent numerical study found a non-negligible nonadiabatic STT for antiferromagnetic domain walls [58], suggesting that electrical currents can control the attenuation of antiferromagnetic SWs.

In addition, a recent experiment on GdFeCo ferrimagnets shows that the adiabatic torque in this material can be large
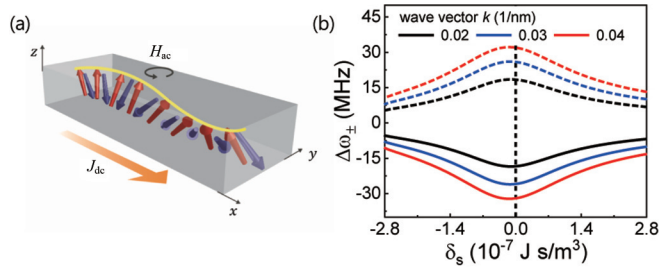
*kjlee@kaist.ac.kr

FIG. 1. (a) A schematic illustration of ferrimagnetic spin waves when the current is applied along the x axis. For numerical simulations, an ac field H_{ac} (10 mT) is applied to excite SWs. (b) The Doppler shift for right- (solid line) and left-handed (dashed line) SW $[\Delta\omega_\pm = \omega_\pm(J = 1 \times 10^9 \text{ A/m}^2) - \omega_\pm(J = 0)]$ as a function of net spin density δ_s. Here, we assume that the exchange constant $A = 3 \times 10^{-12}$ J/m, the easy-axis anisotropy constant along the z direction $K = 10^4$ J/m^3, spin polarization $P_{RE} = 0.1$, $P_{TM} = 0.4$, and the wave vector is 0.02, 0.03, and 0.04 nm^{-1}.

[59], which stems from a finite net spin polarization of RE and TM sublattices. Thus, the current-induced SW Doppler shift of compensated ferrimagnets is expected to be similar in magnitude to that of ferromagnets. Moreover, the same experiment [59] shows that the nonadiabatic torque in this material is large (i.e., equivalently, the ratio of nonadiabaticity β to damping α is large). This large nonadiabaticity of spin current in compensated ferrimagnets is attributed to the enhanced spin mistracking [46,48,58,59], originating from the weakened spin dephasing in the antiferromagnetically aligned spin moments [60,61]. This unique STT characteristic of compensated ferrimagnets motivates us to investigate STT effects on ferrimagnetic SWs.

In this work, we theoretically and numerically study the STT-induced control of ferrimagnetic SW dynamics near the angular momentum compensation point. To begin with, we derive the equations of motion for ferrimagnetic SWs in the presence of two torque components. From the equations of motion, we obtain current-driven ferrimagnetic SW Doppler shift and attenuation. Then, we perform atomistic lattice model simulations to verify the obtained analytic solutions. We show that the ferrimagnetic SW Doppler shift due to the adiabatic torque for right-handed SWs is opposite to that for left-handed SWs since they carry opposite spin polarizations. We also find that the SW attenuation is suppressed, and the SW amplitude is even amplified when a sufficiently large nonadiabatic torque is exerted.

II. ANALYTIC THEORY

We consider a ferrimagnet consisting of RE and TM moments, which are antiferromagnetically coupled as shown in Fig. 1(a). We introduce two unit vectors $\mathbf{A}_k$ and $\mathbf{B}_k$ denoting localized spins located at two sublattices, the A and B sites. We define the total magnetization vector and the staggered magnetization vector as $\mathbf{m} = \mathbf{A}_k + \mathbf{B}_k$ and $\mathbf{n} = (\mathbf{A}_k - \mathbf{B}_k)/2$, respectively. The spin density is $s_{A(B)} = M_{A(B)}/\gamma_{A(B)}$ where $M_{A(B)}$ is the saturation magnetization and $\gamma_{A(B)}$ is the gyromagnetic ratio. The Lagrangian density $\mathcal{L}$ for ferrimagnets is given by [30,62–65]

$$\mathcal{L} = -s\dot{\mathbf{n}} \cdot (\mathbf{n} \times \mathbf{m}) - \delta_s \mathbf{a}(\mathbf{n}) \cdot \dot{\mathbf{n}} - \mathcal{U}, \quad (1)$$

where $s = (s_A + s_B)/2$ is the sum of spin densities of two sublattices, $\delta_s = s_A - s_B$ is the net spin density, $\mathbf{a}(\mathbf{n})$ is the vector potential, and the potential energy $\mathcal{U}$ contains the exchange energy and easy-axis anisotropy energy, given by

$$\mathcal{U} = \frac{A}{2}(\nabla\mathbf{n})^2 + \frac{a}{2}\mathbf{m}^2 + L\mathbf{m} \cdot \partial_x\mathbf{n} - \frac{K}{2}(\hat{\mathbf{z}} \cdot \mathbf{n})^2. \quad (2)$$

Here A is the inhomogeneous exchange, a is the homogeneous exchange, L is the parity-breaking exchange term [65,66], and K is the effective easy-axis anisotropy including the demagnetization effect in the z direction. We assume that the Gilbert damping constant α is the same regardless of site ($\alpha_A = \alpha_B$), which simplifies the Rayleigh dissipation function as $\mathcal{R} = \alpha s\dot{\mathbf{n}}^2$. In this theory, we neglect nonlocal dipolar interaction because net magnetization is an order of magnitude smaller than the ferromagnets.

By solving the above equations for $\mathbf{n}$ and $\mathbf{m}$, we obtain two staggered equations of motion to linear order in the current-induced STT effective field (i.e., by working within linear-response theory) and to the first order in the net magnetization $|\mathbf{m}|$ by assuming that a change from a ground state (with $\mathbf{m} = 0$) is small, i.e., $|\mathbf{m}| \ll 1$, due to the strong antiferromagnetic exchange coupling by following the approach taken in Ref. [67]:

$$\dot{\mathbf{n}} = -\frac{1}{s}\mathbf{f_m} \times \mathbf{n} + \mathbf{T}^{\mathbf{n}}_{STT}, \quad (3)$$

$$\dot{\mathbf{m}} = -\frac{1}{s}\mathbf{f_n} \times \mathbf{n} + 2\alpha\dot{\mathbf{n}} \times \mathbf{n} - \frac{\delta_s}{s}\dot{\mathbf{n}} + \mathbf{T}^{\mathbf{m}}_{STT}, \quad (4)$$

where $\mathbf{f_m} = -\frac{\partial\mathcal{U}}{\partial\mathbf{m}}$, $\mathbf{f_n} = -\frac{\partial\mathcal{U}}{\partial\mathbf{n}}$, $\mathbf{T}^{\mathbf{n(m)}}_{STT}$ is the STT that affects $\mathbf{n}$ ($\mathbf{m}$) dynamics, given as (see Appendix)

$$\mathbf{T}^{\mathbf{n}}_{STT} = -\frac{b_j^+}{2}\frac{\partial\mathbf{n}}{\partial x} - \frac{\beta b_j^-}{2}\mathbf{n} \times \frac{\partial\mathbf{n}}{\partial x}, \quad (5)$$

$$\mathbf{T}^{\mathbf{m}}_{STT} = -b_j^-\frac{\partial\mathbf{n}}{\partial x} - \beta b_j^+\mathbf{n} \times \frac{\partial\mathbf{n}}{\partial x}, \quad (6)$$

where $b_j^\pm = -\frac{\mu_B}{2e}(P_A\frac{g_A}{M_A} \pm P_B\frac{g_B}{M_B})J_e$ is the magnitude of adiabatic spin torque, P_A (P_B) is the spin polarization, g_A (g_B) is the Landé g factor, μ_B is the Bohr magneton, e is the electron charge, J_e is the current density, and β is the nonadiabaticity. Note that, when the two sublattices are equivalent and thus $b_j^- = 0$, Eqs. (5) and (6) are same (except for numerical factors) as the two spin-transfer torque terms for antiferromagnets shown in Eqs. (5) and (6) of Ref. [67]. When deriving Eqs. (5) and (6), we retained the terms involving the gradient of the order parameter $\mathbf{n}$ while neglecting the terms involving the small net magnetization $\mathbf{m}$ by assuming $\mathbf{m}$ is strongly suppressed by the antiferromagnetic exchange coupling. Here, we define that all of spin polarization, Landé g factor, Bohr magneton, and electron charge are positive and assume $\beta_A = \beta_B = \beta$ for simplicity. We note that b_j^+ corresponds to a staggered torque exerting on two sublattice moments, whereas b_j^- corresponds to a uniform torque. For antiferromagnets, b_j^- vanishes and b_j^+ is the only torque to drive dynamics of antiferromagnetic spin textures. In contrast, for ferrimagnets,

both b_j^+ and b_j^- are nonzero in general so that both torques affect the dynamics.

We derive the equation of motion by inserting the STT [Eqs. (5) and (6)] into the staggered equations of motion [Eqs. (3) and (4)]. Then, we obtain the equation of motion for **n** as

$$\rho \mathbf{n} \times \ddot{\mathbf{n}} + 2\alpha s \mathbf{n} \times \dot{\mathbf{n}} + \delta_s \dot{\mathbf{n}}$$
$$= A^* \mathbf{n} \times \partial_x^2 \mathbf{n} + K \mathbf{n} \times n_z \hat{\mathbf{z}} - sb_j^- \partial_x \mathbf{n} - s\beta b_j^+ \mathbf{n} \times \partial_x \mathbf{n}, \quad (7)$$

where $A^* = A - L^2/a$ is the renormalized exchange stiffness constant [65] and $\rho = s^2/a$ is the inertia. It is worthwhile to note that the STT effect, i.e., the third and fourth terms on the right-hand side of Eq. (7), comes from $\mathbf{T}_{\mathrm{STT}}^{\mathbf{m}}$ [Eq. (6)], which is the STT acting on a ferromagnetic component **m**. On the other hand, the contribution of $\mathbf{T}_{\mathrm{STT}}^{\mathbf{n}}$ [Eq. (5)], i.e., the STT acting on a stagger vector **n**, does not appear in Eq. (7) because it is of the third order in small parameters and thus negligible.

By defining a complex field as $\psi_\pm = n_x \mp in_y$ for right- and left-handed SWs and linearizing the above equation for n_x and n_y, we obtain

$$\pm \delta_S \dot{\psi}_\pm - i2\alpha s \dot{\psi}_\pm - i\rho \ddot{\psi}_\pm$$
$$= -iA^* \partial_x^2 \psi_\pm + iK \psi_\pm \mp sb_j^- \partial_x \psi_\pm + is\beta b_j^+ \partial_x \psi_\pm. \quad (8)$$

The upper (lower) sign corresponds to right- (left-) handed SW. By inserting the plane wave solution $\psi_\pm = \exp[i(kx - \omega_\pm t)] \exp[-x/\Lambda_\pm]$ into Eq. (8), we obtain the SW dispersion and SW attenuation length Λ, given as

$$\omega_\pm = \frac{\pm \delta_s + \sqrt{\delta_s^2 + 4\rho(A^* k^2 + K \mp sb_j^- k)}}{2\rho}, \quad (9)$$

$$\Lambda_\pm = \frac{2A^* k \mp sb_j^-}{s(2\alpha\omega_\pm - \beta b_j^+ k)}. \quad (10)$$

Equations (9) and (10) are our central results.

We first discuss the current-induced SW Doppler shift [Eq. (9)]. For antiferromagnets ($\delta_s = 0$ and $b_j^- = 0$), Eq. (9) shows no current-induced SW Doppler shift. This is caused by the fact that we derive the equations with the second-order expansion of small parameters. When we consider up to the third-order terms, there is a finite SW Doppler shift even for antiferromagnets, which is consistent with Ref. [57]. For ferrimagnets, the last term in the square root of Eq. (9) (i.e., $\mp sb_j^- k$) signifies the current-induced SW Doppler shift. It originates from the uniform adiabatic torque b_j^- acting on a ferromagnetic component **m**.

Figure 1(b) shows the current-induced SW Doppler shift $\Delta\omega_\pm$ as a function of the net spin density δ_s, computed from Eq. (9). Three observations are worth mentioning. First, the sign of Doppler shift depends on the SW handedness because opposite spin polarizations are carried by right- and left-handed SWs. Second, the Doppler shift is also related to the sign of b_j^- because b_j^- can be positive or negative depending on the material parameters such as polarization, Landé g factor, and saturation magnetization. For a specific RE-TM ferrimagnet, i.e., a GdCo ferrimagnet, the sign of b_j^- would not change with temperature in the vicinity of T_A because $g_{\mathrm{Gd}} \approx g_{\mathrm{Co}}$ and M_{Gd} is not much different from M_{Co} [59],

while P_{Gd} is four times smaller than than P_{Co} [68]. Third, the Doppler shift $\Delta\omega_\pm$ is maximized in the vicinity of the angular momentum compensation point T_A (i.e., $\delta_s = 0$). To get an insight into the second observation, we expand Eq. (9) in the limit of small current density and obtain $\omega_\pm \approx \omega_{0,\pm} + \Delta\omega_\pm$, where the current-independent frequency ω_0 is given by

$$\omega_{0,\pm} = \frac{\pm \delta_s + \sqrt{\delta_s^2 + 4\rho(A^* k^2 + K)}}{2\rho}, \quad (11)$$

and, the current-induced Doppler shift $\Delta\omega_\pm$ is given by

$$\Delta\omega_\pm = \mp \frac{sb_j^- k}{\sqrt{\delta_s^2 + 4\rho(A^* k^2 + K)}}. \quad (12)$$

Equation (12) shows that, in this limit, the current-induced Doppler shift of ferrimagnetic SW is linear in k and in current density as for ferromagnetic SWs [52–54]. It also shows that the current-induced Doppler shift $\Delta\omega_\pm$ is maximized in the vicinity of T_A where δ_s vanishes. This result suggests that one can experimentally determine T_A by measuring the current-induced SW Doppler shift.

We next discuss the current-induced control of SW attenuation [Eq. (10)]. For antiferromagnets ($\delta_s = 0$ and $b_j^- = 0$), Eq. (10) shows that the staggered nonadiabatic torque (i.e., $\beta b_j^+ k$) modifies the SW attenuation length. It means that the SW attenuation length in antiferromagnets is determined by the denominator ($2\alpha\omega_\pm - \beta b_j^+ k$), which describes the competition between the damping torque and the staggered nonadiabatic torque. For ferrimagnets, in addition to the staggered nonadiabatic torque, the uniform adiabatic torque (i.e., $\mp sb_j^-$) in the numerator of Eq. (10) also controls the SW attenuation length, but its contribution is independent of k. With typical material parameters, however, this adiabatic-torque contribution to the SW attenuation length is usually negligible so that the main contribution is the competition between the damping torque and the staggered nonadiabatic torque, even for ferrimagnets.

Current-induced effect on the SW attenuation length depends on the relative flow direction of the electron and the SW (k). Considering $\beta > 0$, when electrons flow in the same (opposite) direction as SWs, the attenuation length increases (decreases). When a large current is injected, i.e., $b_j^+ > \frac{2\alpha\omega_\pm}{\beta k}$, Eq. (10) becomes negative so that the SW solution is $\psi = \exp[i(kx - \omega t)] \exp[+x/|\Lambda|]$, meaning that SWs are amplified for both antiferromagnets and ferrimagnets.

III. NUMERICAL ANALYSIS

To verify the above analytic results, we perform atomistic lattice model simulations. We consider the one-dimensional atomistic Hamiltonian as

$$\mathcal{H} = A_{\mathrm{sim}} \sum_{i,j} \mathbf{S}_i \cdot \mathbf{S}_j - K_{\mathrm{sim}} \sum_i (\mathbf{S}_i \cdot \hat{\mathbf{z}})^2, \quad (13)$$

where A_{sim} is the exchange constant, K_{sim} is the easy-axis anisotropy constant, S_i is the spin moment vector at the i site, and j is the notation representing the nearest lattice of the site i. The atomistic Landau-Lifshitz-Gilbert equation including

TABLE I. The saturation magnetizations for RE and TM elements. The index T_2 corresponds to the angular momentum compensation temperature T_A.

Index	T_1	$T_2 (= T_A)$	T_3
M_{RE} (kA/m)	426	386	344
M_{TM} (kA/m)	455	424.6	392
$\delta_s (\times 10^{-8}$ J s/m^3)	7.02	0	−7.02

STT terms is given as

$$\frac{\partial \mathbf{S}_i}{\partial t} = -\gamma_i \mu_0 \mathbf{S}_i \times \mathbf{H}_{\text{eff},i} + \alpha_i \mathbf{S}_i \times \frac{\partial \mathbf{S}_i}{\partial t} - b_{J,i} \frac{\mathbf{S}_{i+1} - \mathbf{S}_{i-1}}{2d}$$

$$- \beta_i b_{J,i} \mathbf{S}_i \times \frac{\mathbf{S}_{i+1} - \mathbf{S}_{i-1}}{2d}. \quad (14)$$

We solve the above equation by using the Runge-Kutta fourth-order method. Here, $\gamma_i = g_i \mu_B / \hbar$ is the gyromagnetic ratio, μ_0 is the permeability in vacuum, g_i is the Landé g factor, $\mathbf{H}_{\text{eff},i} = -\frac{1}{\mu_i} \frac{\partial \mathcal{H}}{\partial \mathbf{S}_i}$ is the effective field, μ_i is the magnetic moment, α_i is the Gilbert damping constant, $b_{J,i} = -\frac{g_i P_i \mu_B}{2eM_i} J_e$ is the magnitude of adiabatic STT, P_i is the spin polarization, M_i is the saturation magnetization, and β_i is the nonadiabaticity. We locally apply a circularly polarized external field, $\mu_0 \mathbf{H}_{ac} = \mu_0 H_0 (\cos 2\pi f t, \sin 2\pi f t, 0)$ with $\mu_0 H_0 = 10$ mT to excite SWs in a ferrimagnet. We also inject an in-plane current corresponding to the current density J_e ranging from -5×10^{12} A/m^2 to $+5 \times 10^{12}$ A/m^2 to induce STT. We use the following simulation parameters: the lattice constant $d = 0.4$ nm, the exchange constant $A_{\text{sim}} = 7.5$ meV, the easy-axis anisotropy constant $K_{\text{sim}} = 0.004$ meV, the Gilbert damping constant $\alpha = 0.003$, the nonadiabaticity $\beta = 10\alpha$ and $\beta = 100\alpha$, the Landé g factor $g_{RE} = 2$, $g_{TM} = 2.2$, and the spin polarization $P_{RE} = 0.1$, $P_{TM} = 0.4$. In the continuum limit, the corresponding parameters in Eq. (7) are given by $A^* = 4A_{\text{sim}}/d$ and $K = 4K_{\text{sim}}/d^3$. We assume that both damping constant and nonadiabaticity are the same regardless of the sublattice site as assumed for the analytic theory. We use the saturation magnetization listed in Table I, which is measured in Ref. [59] for GdFeCo. We consider the system size of $3200 \times 100 \times 0.4$ nm^3 with cell size $0.4 \times 100 \times 0.4$ nm^3 and perform simulations up to 4 ns, after which the system reaches a sufficiently steady state.

Figures 2(a) and 2(b), respectively, show dispersions of the right- and left-handed SWs at zero applied current. T_2 corresponds to the angular momentum compensation point T_A where $\delta_s = S_{RE} - S_{TM} = 0$ and $T_1 < T_2 < T_3$. In all cases, numerical results (symbols) are in agreement with analytical results [lines, Eq. (9)]. The frequency of the right-handed SW is the highest at T_1 [Fig. 2(a)], whereas the frequency of the left-handed SW is the lowest at T_1 [Fig. 2(b)]. This difference originates from different δ_s [Eq. (9)].

Figures 2(c) and 2(d), respectively, show the current-induced SW Doppler shifts of the right- and left-handed SWs at the angular momentum compensation temperature $T_A (= T_2)$ when the current density $J_e = \pm 5 \times 10^{12}$ A/m^2 is applied. Numerical results (symbols) are in reasonable agreement with Eq. (9) (solid lines). For the right-handed SW [Fig. 2(c)] and $k > 0$, a positive (negative) current decreases
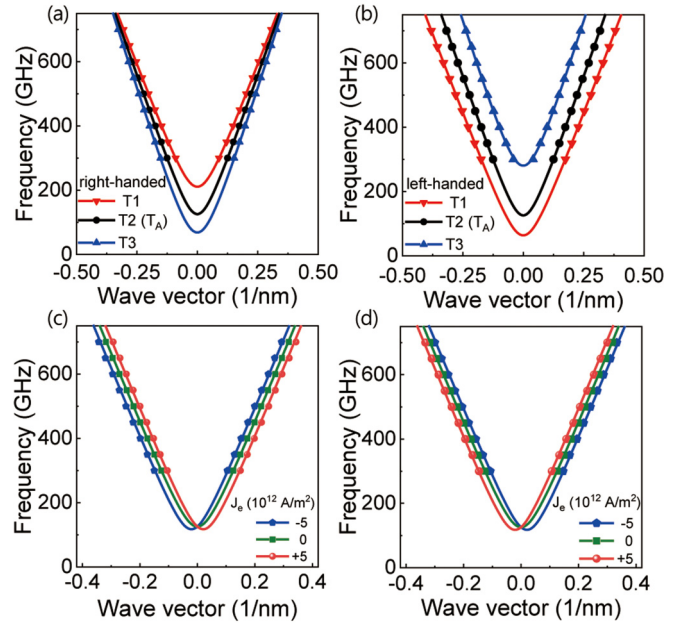

FIG. 2. Ferrimagnetic SW dispersion for (a) right- and (b) left-handed SW in the vicinity of angular momentum compensation temperature (T_A) when no current is applied. Current-induced Doppler shift of (c) right- and (d) left-handed SWs in ferrimagnet at T_A.

(increases) the SW frequency. On the other hand, for the left-handed SW [Fig. 2(d)] and $k > 0$, a positive (negative) current increases (decreases) the SW frequency. Therefore, the sign of the Doppler shift of the right-handed SW is opposite to that of the left-handed SW, consistent with the analytic expression [Eq. (9)]. The same tendency of Doppler shift is obtained for other temperatures (not shown).

Figures 3(a) [3(b)] shows the SW attenuation length as a function of the current density for $\beta = 10\alpha$ and right-(left-)handed SWs. The SW frequency ($\omega/2\pi$) is 0.4 THz. Numerical results (symbols) are in reasonable agreement with Eq. (10) (solid lines). For a positive β, we find that the SW attenuation length of both right- and left-handed SWs increases when electrons move in the same direction with the SW propagation. When the nonadiabatic torque is sufficiently large [$\beta = 100\alpha$, Figs. 3(c) and 3(d)], the antidamping effect of nonadiabatic torque overcomes the intrinsic damping torque and, as a result, the SW attenuation length becomes negative, meaning that the SW is amplified.

IV. SUMMARY

To summarize, we theoretically study the STT effects on ferrimagnetic SWs. Unlike antiferromagnetic SWs for which current-induced Doppler shift is small, ferrimagnetic SWs exhibit non-negligible Doppler shift because of a finite spin polarization. The current-induced Doppler shift is maximized in the vicinity of the angular momentum compensation point T_A, providing a way to measure T_A. The sign of the Doppler shift depends on the SW handedness, because the spin polarization carried by SWs also depends on the SW handedness. A recent experiment has identified the SW handedness in
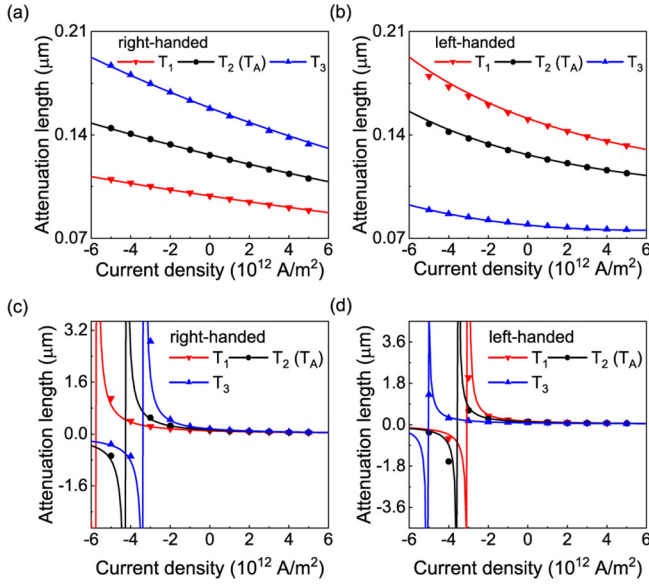
FIG. 3. The SW attenuation length as a function of current density at $\beta = 10\alpha$ for (a), (b) and $\beta = 100\alpha$ for (c), (d). (a), (c) are for right-handed SWs and (b), (d) are for left-handed SWs. The solid lines are analytic results and symbols are numerical results.

ferrimagnets by measuring the relative magnitudes of Stokes and anti-Stokes peak in the Brillouin light scattering [39]. Our work suggests an alternative way to identify the SW handedness by measuring the sign of current-induced SW Doppler shift.

It is found that the attenuation length of ferrimagnetic SWs is modified by nonadiabatic staggered torque, which can be used to experimentally determine the nonadiabaticity β of a ferrimagnet. Combined with the current-induced SW Doppler shift, our work provides a way to simultaneously determine important material parameters of ferrimagnets, namely, the angular momentum compensation point T_A, the spin polarization P, and the nonadiabaticity β, by performing a single series of time-domain measurements of current-induced SW dynamics in a ferrimagnet. However, the determination of the handedness or the unknown parameters is experimentally challenging and may need to be combined with other independent measurements of the spin polarization [68] and T_A [29].

ACKNOWLEDGMENTS

APPENDIX: DERIVATION OF EXPRESSION FOR STT ON FERRIMAGNETS

In this part, we derive Eqs. (5) and (6) from the STT exerting on each sublattice as

$$\frac{\partial \mathbf{A}_k}{\partial t} = -b_{j,\mathbf{A}}\frac{\partial \mathbf{A}_k}{\partial x} - \beta_{\mathbf{A}} b_{j,\mathbf{A}} \mathbf{A}_k \times \frac{\partial \mathbf{A}_k}{\partial x}, \quad (A1)$$

$$\frac{\partial \mathbf{B}_k}{\partial t} = -b_{j,\mathbf{B}}\frac{\partial \mathbf{B}_k}{\partial x} - \beta_{\mathbf{B}} b_{j,\mathbf{B}} \mathbf{B}_k \times \frac{\partial \mathbf{B}_k}{\partial x}, \quad (A2)$$

where $b_{j,i} = -\frac{g_i \mu_B P_i}{2eM_i} J_e$ and the first (second) term represents the adiabatic (nonadiabatic) torque. Using $\mathbf{A}_k = \frac{\mathbf{m}}{2} + \mathbf{n}$ and $\mathbf{B}_k = \frac{\mathbf{m}}{2} - \mathbf{n}$, we obtain

$$\frac{\partial}{\partial t}\left(\frac{\mathbf{m}}{2} + \mathbf{n}\right) = -b_{j,\mathbf{A}}\frac{\partial}{\partial x}\left(\frac{\mathbf{m}}{2} + \mathbf{n}\right) - \beta_{\mathbf{A}} b_{j,\mathbf{A}}\left(\frac{\mathbf{m}}{2} + \mathbf{n}\right)$$
$$\times \frac{\partial}{\partial x}\left(\frac{\mathbf{m}}{2} + \mathbf{n}\right), \quad (A3)$$

$$\frac{\partial}{\partial t}\left(\frac{\mathbf{m}}{2} - \mathbf{n}\right) = -b_{j,\mathbf{B}}\frac{\partial}{\partial x}\left(\frac{\mathbf{m}}{2} - \mathbf{n}\right) - \beta_{\mathbf{B}} b_{j,\mathbf{B}}\left(\frac{\mathbf{m}}{2} - \mathbf{n}\right)$$
$$\times \frac{\partial}{\partial x}\left(\frac{\mathbf{m}}{2} - \mathbf{n}\right). \quad (A4)$$

Combining Eqs. (A3) and (A4) and assuming a uniform β, we obtain

$$\frac{\partial \mathbf{n}}{\partial t} = -\frac{b_j^-}{4}\frac{\partial \mathbf{m}}{\partial x} - \frac{b_j^+}{2}\frac{\partial \mathbf{n}}{\partial x} - \frac{\beta b_j^-}{8}\mathbf{m} \times \frac{\partial \mathbf{m}}{\partial x} - \frac{\beta b_j^+}{4}\mathbf{m}$$
$$\times \frac{\partial \mathbf{n}}{\partial x} - \frac{\beta b_j^+}{4}\mathbf{n} \times \frac{\partial \mathbf{m}}{\partial x} - \frac{\beta b_j^-}{2}\mathbf{n} \times \frac{\partial \mathbf{n}}{\partial x}, \quad (A5)$$

$$\frac{\partial \mathbf{m}}{\partial t} = -\frac{b_j^+}{2}\frac{\partial \mathbf{m}}{\partial x} - b_j^-\frac{\partial \mathbf{n}}{\partial x} - \frac{\beta b_j^+}{4}\mathbf{m} \times \frac{\partial \mathbf{m}}{\partial x} - \frac{\beta b_j^-}{2}\mathbf{m}$$
$$\times \frac{\partial \mathbf{n}}{\partial x} - \frac{\beta b_j^-}{2}\mathbf{n} \times \frac{\partial \mathbf{m}}{\partial x} - \beta b_j^+\mathbf{n} \times \frac{\partial \mathbf{n}}{\partial x}, \quad (A6)$$

where $b_j^\pm = -\frac{\mu_B}{2e}(P_A \frac{g_A}{M_A} \pm P_B \frac{g_B}{M_B})J_e$. By retaining the terms involving the gradient of the order parameter $\mathbf{n}$ while neglecting the terms involving the small net magnetization $\mathbf{m}$ by assuming that $\mathbf{m}$ is strongly suppressed by the antiferromagnetic exchange coupling and thus $|\mathbf{m}| \ll 1$, the staggered equations of STT are given as

$$\mathbf{T}_{\text{STT}}^{\mathbf{n}} = -\frac{b_j^+}{2}\frac{\partial \mathbf{n}}{\partial x} - \frac{\beta b_j^-}{2}\mathbf{n} \times \frac{\partial \mathbf{n}}{\partial x}, \quad (A7)$$

$$\mathbf{T}_{\text{STT}}^{\mathbf{m}} = -b_j^-\frac{\partial \mathbf{n}}{\partial x} - \beta b_j^+\mathbf{n} \times \frac{\partial \mathbf{n}}{\partial x}. \quad (A8)$$

[1] A. A. Serga, A. V. Chumak, and B. Hillebrands, J. Phys. D **43**, 264002 (2010).

[2] V. V. Kruglyak, S. O. Demokritov, and D. Grundler, J. Phys. D **43**, 264001 (2010).

[3] B. Lenk, H. Ulrichs, F. Garbs, and M. Münzenberg, Phys. Rep. **507**, 107 (2011).

[4] A. Khitun and K. L. Wang, Superlattices Microstruct. **38**, 184 (2005).

[5] T. Schneider, A. A. Serga, B. Leven, and B. Hillebrands, Appl. Phys. Lett. **92**, 022505 (2008).

[6] K.-S. Lee and S.-K. Kim, J. Appl. Phys. **104**, 053909 (2008).

[7] A. Khitun, M. Bao, and K. L. Wang, J. Phys. D **43**, 264005 (2010).

[8] A. Khitun, J. Appl. Phys. **111**, 054307 (2012).

[9] N. Sato, K. Sekiguchi, and Y. Nozaki, Appl. Phys. Express **6**, 063001 (2013).

[10] M. Jamali, J. H. Kwon, S.-M. Seo, K.-J. Lee, and H. Yang, Sci. Rep. **3**, 3160 (2013).

[11] G. Csaba, A. Papp, and W. Porod, J. Appl. Phys. **115**, 17C741 (2014).

[12] K. Vogt, F. Y. Fradin, J. E. Pearson, T. Sebastian, S. D. Bader, B. Hillebrands, A. Hoffmann, and H. Schultheiss, Nat. Commun. **5**, 3727 (2014).

[13] A. V. Chumak, V. I. Vasyuchka, A. A. Serga, and B. Hillebrands, Nat. Phys. **11**, 453 (2015).

[14] M. Vogel, A. V. Chumak, E. H. Waller, T. Langner, V. I. Vasyuchka, B. Hillebrands, and G. V. Freymann, Nat. Phys. **11**, 487 (2015).

[15] A. Haldar, D. Kumar, and A. O. Adeyeye, Nat. Nanotechnol. **11**, 437 (2016).

[16] J. H. Kwon, J. Yoon, P. Deorani, J. M. Lee, J. Sinha, K.-J. Lee, M. Hayashi, and H. Yang, Sci. Adv. **2**, e1501892 (2016).

[17] K. Sekiguchi, S.-W. Lee, H. Sukegawa, N. Sato, S.-H. Oh, R. D. McMichael, and K.-J. Lee, npg Asia Mater. **9**, e392 (2017).

[18] J. Nishitani, K. Kozuki, T. Nagashima, and M. Hangyo, Appl. Phys. Lett. **96**, 221906 (2010).

[19] T. Kampfrath, A. Sell, G. Klatt, A. Pashkin, S. Mährlein, T. Dekorsy, M. Wolf, M. Fiebig, A. Leitenstorfer, and R. Huber, Nat. Photonics **5**, 31 (2011).

[20] F. Keffer and C. Kittel, Phys. Rev. **85**, 329 (1952).

[21] R. A. Duine, K.-J. Lee, S. S. P. Parkin, and M. D. Stiles, Nat. Phys. **14**, 217 (2018).

[22] R. Cheng, M. W. Daniels, J.-G. Zhu, and D. Xiao, Sci. Rep. **6**, 24223 (2016).

[23] J. Lan, W. Yu, and J. Xiao, Nat. Commun. **8**, 178 (2017).

[24] W. Yu, J. Lan, and J. Xiao, Phys. Rev. B **98**, 144422 (2018).

[25] S.-J. Lee, D.-K. Lee, and K.-J. Lee, Phys. Rev. B **101**, 064422 (2020).

[26] W. Yu, J. Lan, and J. Xiao, Phys. Rev. Appl. **13**, 024055 (2020).

[27] C. D. Stanciu, A. V. Kimel, F. Hansteen, A. Tsukamoto, A. Itoh, A. Kirilyuk, and Th. Rasing, Phys. Rev. B **73**, 220402(R) (2006).

[28] T. Satoh, Y. Terui, R. Moriya, B. A. Ivanov, K. Ando, E. Saitoh, T. Shimura, and K. Kuroda, Nat. Photonics **6**, 662 (2012).

[29] K.-J. Kim, S. K. Kim, Y. Hirata, S.-H. Oh, T. Tono, D.-H. Kim, T. Okuno, W. S. Ham, S. Kim, G. Go, Y. Tserkovnyak, A. Tsukamoto, T. Moriyama, K.-J. Lee, and T. Ono, Nat. Mater. **16**, 1187 (2017).

[30] S.-H. Oh, S. K. Kim, D.-K. Lee, G. Go, K.-J. Kim, T. Ono, Y. Tserkovnyak, and K.-J. Lee, Phys. Rev. B **96**, 100407(R) (2017).

[31] S. K. Kim, K.-J. Lee, and Y. Tserkovnyak, Phys. Rev. B **95**, 140404(R) (2017).

[32] L. Caretta, M. Mann, F. Büttner, K. Ueda, B. Pfau, C. M. Günther, P. Hessing, A. Churikova, C. Klose, M. Schneider, D. Engel, C. Marcus, D. Bono, K. Bagschik, S. Eisebitt, and G. S. D. Beach, Nat. Nanotechnol. **13**, 1154 (2018).

[33] S. A. Siddiqui, J. Han, J. T. Finley, C. A. Ross, and L. Liu, Phys. Rev. Lett. **121**, 057701 (2018).

[34] Y. Hirata, D.-H. Kim, S. K. Kim, D.-K. Lee, S.-H. Oh, D.-Y. Kim, T. Nishimura, T. Okuno, Y. Futakawa, H. Yoshikawa, A. Tsukamoto, Y. Tserkovnyak, Y. Shiota, T. Moriyama, S.-B. Choe, K.-J. Lee, and T. Ono, Nat. Nanotechnol. **14**, 232 (2019).

[35] S.-H. Oh, S. K. Kim, J. Xiao, and K.-J. Lee, Phys. Rev. B **100**, 174403 (2019).

[36] D.-H. Kim, T. Okuno, S. K. Kim, S.-H. Oh, T. Nishimura, Y. Hirata, Y. Futakawa, H. Yoshikawa, A. Tsukamoto, Y. Tserkovnyak, Y. Shiota, T. Moriyama, K.-J. Kim, K.-J. Lee, and T. Ono, Phys. Rev. Lett. **122**, 127203 (2019).

[37] T. Okuno, S. K. Kim, T. Moriyama, D.-H. Kim, H. Mizuno, T. Ikebuchi, Y. Hirata, H. Yoshikawa, A. Tsukamoto, K.-J. Kim, Y. Shiota, K.-J. Lee, and T. Ono, Appl. Phys. Express **12**, 093001 (2019).

[38] S. Funada, T. Nishimura, Y. Shiota, S. Kasukawa, M. Ishibashi, T. Moriyama, and T. Ono, Jpn. J. Appl. Phys. **58**, 080909 (2019).

[39] C. Kim, S. Lee, H.-G. Kim, J.-H. Park, K.-W. Moon, J. Y. Park, J. M. Yuk, K.-J. Lee, B.-G. Park, S. K. Kim, K.-J. Kim, and C. Hwang, Nat. Mater. **19**, 980 (2020).

[40] J. Shim, S.-J. Kim, S. K. Kim, and K.-J. Lee, Phys. Rev. Lett. **125**, 027205 (2020).

[41] J. C. Slonczewski, J. Magn. Magn. Mater. **159**, L1 (1996).

[42] L. Berger, Phys. Rev. B **54**, 9353 (1996).

[43] G. Tatara and H. Kohno, Phys. Rev. Lett. **92**, 086601 (2004).

[44] S. Zhang and Z. Li, Phys. Rev. Lett. **93**, 127204 (2004).

[45] A. Thiaville, Y. Nakatani, J. Miltat, and Y. Suzuki, Europhys. Lett. **69**, 990 (2005).

[46] J. Xiao, A. Zangwill, and M. D. Stiles, Phys. Rev. B **73**, 054428 (2006).

[47] Y. Tserkovnyak, H. J. Skadsem, A. Brataas, and G. E. W. Bauer, Phys. Rev. B **74**, 144405 (2006).

[48] G. Tatara, H. Kohno, J. Shibata, Y. Lemaho, and K.-J. Lee, J. Phys. Soc. Jpn. **76**, 054707 (2007).

[49] I. Garate, K. Gilmore, M. D. Stiles, and A. H. MacDonald, Phys. Rev. B **79**, 104416 (2009).

[50] K.-J. Lee, M. D. Stiles, H.-W. Lee, J.-H. Moon, K.-W. Kim, and S.-W. Lee, Phys. Rep. **531**, 89 (2013).

[51] K.-W. Kim, K.-J. Lee, H.-W. Lee, and M. D. Stiles, Phys. Rev. B **92**, 224426 (2015).

[52] P. Lederer and D. L. Mills, Phys. Rev. **148**, 542 (1966).

[53] V. Vlaminck and M. Bailleul, Science **322**, 410 (2008).

[54] S.-M. Seo, K.-J. Lee, H. Yang, and T. Ono, Phys. Rev. Lett. **102**, 147202 (2009).

[55] K. Sekiguchi, K. Yamada, S.-M. Seo, K.-J. Lee, D. Chiba, K. Kobayashi, and T. Ono, Phys. Rev. Lett. **108**, 017203 (2012).

[56] J.-Y. Chauleau, H. G. Bauer, H. S. Körner, J. Stigloher, M. Härtinger, G. Woltersdorf, and C. H. Back, Phys. Rev. B **89**, 020403(R) (2014).

[57] A. C. Swaving and R. A. Duine, Phys. Rev. B. **83**, 054428 (2011).

[58] H.-J. Park, Y. Jeong, S.-H. Oh, G. Go, J. H. Oh, K.-W. Kim, H.-W. Lee, and K.-J. Lee, Phys. Rev. B **101**, 144431 (2020).

[59] T. Okuno, D.-H. Kim, S.-H. Oh, S. K. Kim, Y. Hirata, T. Nishimura, W. S. Ham, Y. Futakawa, H. Yoshikawa, A. Tsukamoto, Y. Tserkovnyak, Y. Shiota, T. Moriyama, K.-J. Kim, K.-J. Lee, and T. Ono, Nat. Electron. **2**, 389 (2019).

[60] J. Yu, D. Bang, R. Mishra, R. Ramaswamy, J. H. Oh, H.-J. Park, Y. Jeong, P. V. Thach, D.-K. Lee, G. Go, S.-W. Lee, Y. Wang, S. Shi, X. Qiu, H. Awano, K.-J. Lee, and H. Yang, Nat. Mater. **18**, 29 (2019).

[61] Y. Lim, B. Khodadadi, J.-F. Li, D. Viehland, A. Manchon, and S. Emori, arXiv:2001.06918 [Phys. Rev. B (to be published)].

[62] A. F. Andreev and V. I. Marchenko, Sov. Phys. - Usp. **23**, 21 (1980).

[63] B. A. Ivanov and A. L. Sukstanskii, Solid State Commun. **50**, 523 (1984).

[64] E. G. Tveten, A. Qaiumzadeh, and A. Brataas, Phys. Rev. Lett. **112**, 147204 (2014).

[65] E. G. Tveten, T. Müller, J. Linder, and A. Brataas, Phys. Rev. B **93**, 104408 (2016).

[66] N. Papanicolaou, Phys. Rev. B **51**, 15062 (1995).

[67] K. M. D. Hals, Y. Tserkovnyak, and A. Brataas, Phys. Rev. Lett. **106**, 107206 (2011).

[68] C. Kaiser, A. F. Panchula, and S. S. P. Parkin, Phys. Rev. Lett. **95**, 047202 (2005).